Available online at www.sciencedirect.com
SCIENCE DIRECT®
Nuclear Instruments and Methods in Physics Research A 547 (2005) 50–55
NUCLEAR INSTRUMENTS & METHODS IN PHYSICS RESEARCH Section A
www.elsevier.com/locate/nima

Development of hard X-ray photoelectron spectroscopy at BL29XU in SPring-8

Y. Takata[a,*], M. Yabashi[b,c], K. Tamasaku[b], Y. Nishino[b], D. Miwa[b], T. Ishikawa[b,c], E. Ikenaga[c], K. Horiba[a], S. Shin[a,d], M. Arita[e], K. Shimada[e], H. Namatame[e], M. Taniguchi[e], H. Nohira[f], T. Hattori[f], S. Södergren[g], B. Wannberg[g], K. Kobayashi[c]

[a]*Soft X-ray Spectroscopy Laboratory, RIKEN/SPring-8, 1-1-1 Kouto, Mikazuki-cho, Sayo-gun, Hyogo 679-5148, Japan*
[b]*Coherent X-ray Optics Laboratory, RIKEN/SPring-8, 1-1-1 Kouto, Mikazuki-cho, Sayo-gun, Hyogo 679-5148, Japan*
[c]*JASRI/SPring-8, 1-1-1 Kouto, Mikazuki-cho, Sayo-gun, Hyogo 679-5198, Japan*
[d]*ISSP, University of Tokyo, Kashiwanoha, Kashiwa, Chiba 277-8581, Japan*
[e]*HiSOR, Hiroshima University, Kagamiyama 2-313, Higashi-Hiroshima 739-5826, Japan*
[f]*Department of Electrical and Electronic Engineering, Musashi Institute of Technology, Tamazutsumi 1-28-1, Setagaya-ku, Tokyo 158-8557, Japan*
[g]*Gammadata Scienta AB, P.O. Box 15120, SE-750 15 Uppsala, Sweden*

Available online 6 June 2005

Abstract

We have realized hard X-ray (HX) photoelectron spectroscopy (PES) with high-throughput and high-energy-resolution for core level and valence band studies using high-energy and high-brilliance synchrotron radiation at BL29XU in SPring-8. Large escape depth of high-energy photoelectrons enables us to probe intrinsic bulk states almost free from surface condition. By use of a newly developed electron energy analyzer and well-focused X-rays, high-energy resolution of 75 meV ($E/\Delta E = 79,000$) was realized for 5.95 keV photoelectrons.

PACS: 07.81.+a; 07.85.Qe; 71.20.−b

Keywords: Photoelectron spectroscopy; Bulk probe; Electronic structure; Hard X-ray

1. Introduction

Photoelectron spectroscopy (PES) has been used extensively to experimentally determine the electronic structure of core levels and valence bands

*Corresponding author. Tel.: +81 791 58 2933; fax: +81 791 58 2934.
E-mail address: takatay@spring8.or.jp (Y. Takata).

0168-9002/$ - see front matter © 2005 Elsevier B.V. All rights reserved.
doi:10.1016/j.nima.2005.05.011

(VBs) [1]. However, conventional PES is surface sensitive because of the short inelastic-mean-free-paths (IMFPs) [2]. In order to attain larger probing depths for VBs than that in vacuum ultraviolet spectroscopy, soft X-ray (SX) VB–PES using synchrotron radiation (SR) has recently become attractive [3]. However, it is obvious that SX–PES is still surface sensitive, because the IMFPs of a valence electron are only 1.3 and 2 nm for Au and Si at a kinetic energy (KE) of 1 keV, respectively [2]. In the case of core levels, smaller KEs than those of VBs enhance the surface sensitivity, making it rather difficult to probe the bulk character.

In contrast to the above-mentioned surface-sensitive PES techniques, the IMFP values of a valence electron for Au and Si increase to 5.5 and 9.2 nm, respectively at 6 keV [2], which lies in the range of hard X-rays (HXs). The straightforward way to realize an intrinsic bulk probe is to increase the KE of photoelectrons by use of HXs. The first feasibility test of HX–PES was done by Lindau et al. [4] in 1974 using a first generation SR source; however, the feeble signal intensity even of Au 4f core level excluded the possibility of studies of VBs. What has prevented HX VB–PES from being realized is the rapid decrease in subshell photoionization cross-section (σ) with photon energy. The σ values for Au 5d (1×10^{-5} Mb) and Si 3p (3×10^{-5} Mb) at 6 keV are only 1–2% of those at 1 keV [5].

In order to realize HX–PES with high-energy resolution and high throughput, both high-brilliant SR and high-performance electron energy analyzer are required. After the second generation SR became available, there have been a few reports on core level photoelectron and resonant Auger spectroscopy [6,7] using several keV X-rays. We started development of HX–PES at the third generation SR facility, SPring-8 in 2001 with the aim of studying the electronic structure of solids with high-energy-resolution and high-throughput, especially for VBs. In 2002, we performed a feasibility test of HX–PES at 5.95 keV and confirmed the capability to probe the intrinsic bulk electronic structure of both core levels and VBs [8,9]. HX–PES has also been developed at ESRF [10–12]. All these experimental achievements indicate that HX–PES will contribute significantly to the study of electronic structure of solids [6–12]. The wide range of applications includes depth-resolved electronic structure, buried layers, interfaces, ultrashallow junctions and the bulk electronic structure of strongly correlated electron systems. Here, we describe the characteristics of HX–PES at BL29XU in SPring-8 and the basic performance of our system.

2. Experimental

The essential problem to overcome in HX–PES is the weak signal intensity due to small σ values as pointed out above. Of course, the intensity of X-rays and the detection efficiency of an electron energy analyzer are the critical factors. In addition to these, the configuration of the experimental setup also influences the signal intensity. Fig. 1 shows IMFPs up to a KE of 10 keV for several materials [2]. IMFPs at the KE of 6 keV range from 4 to 15 nm and are almost five times larger than those at 1 keV. However, these values are much smaller than the X-ray attenuation length (30 μm for Si and 1 μm for Au at 6 keV). In order to avoid wasting X-rays by photoionization in the region deeper than the electron escaping depth, grazing incidence of X-rays relative to sample surface is desirable. On the other hand, to achieve a large probing depth, photoelectrons should be

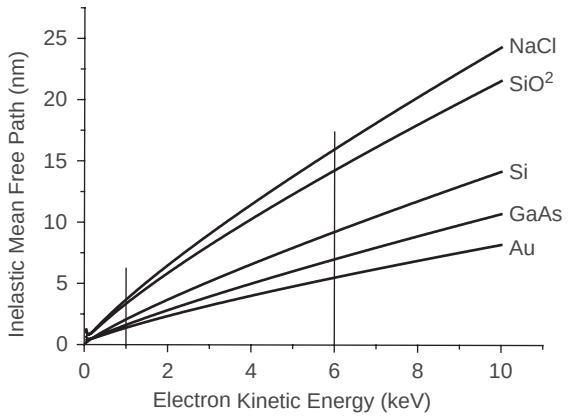

Fig. 1. Inelastic mean free paths for electron kinetic energies up to 10 keV, for Au, GaAs, Si, SiO_2, and NaCl.

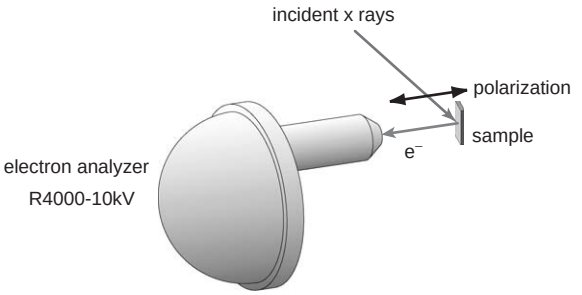

Fig. 2. Schematic of experimental setup. The lens axis of the electron energy analyzer is placed perpendicular to incident X-rays and parallel to the polarization vector. The incidence angle relative to sample surface is typically set to 5°.

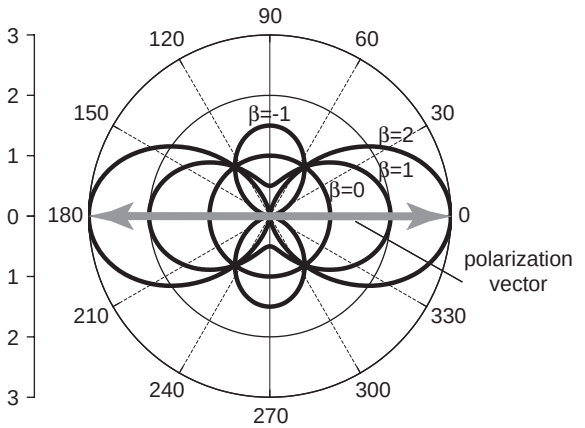

Fig. 3. Angular distribution of photoelectrons from free atoms. For a positive asymmetry parameter β, the intensities have a maximum at the direction of the polarization vector.

detected in the direction close to the normal of the sample surface. Hence, we employed the configuration shown in Fig. 2. The lens axis of the analyzer is placed perpendicular to X-ray beam and the incidence angle relative to the sample surface is typically set to 5°.

Under this configuration, the lens axis is parallel to the polarization vector of X-rays. This relation also plays a role to gain photoelectron intensity. When we use linearly polarized light as an excitation source, photoelectrons from free atoms show angular distribution depending on asymmetry parameter β (see Eq. (5) in Ref. [5]) as shown in Fig. 3. For HX–PES, almost all subshells have positive β values [5] and their intensities have a maximum in the direction parallel to the polarization vector. This behavior is considered applicable even to solids.

Based on these considerations, an HX–PES apparatus has been constructed at the X-ray undulator beamline BL29XU [13,14] in SPring-8. The available photon flux is about 2×10^{11} photons/s with the spot size of 60 (vertical) × 100 (horizontal) μm^2. Fine focus increases considerably the photoelectron intensity because the lens system of our analyzer magnifies the spot size on the sample surface by five times at the entrance slit of the hemispherical analyzer. The band width of X-rays at 5.95 keV is nearly 60 meV (FWHM). Details of X-ray optics for HX–PES is described elsewhere [15]. Fig. 4 shows the picture of the apparatus placed in the experimental hutch at BL 29XU. An electron energy analyzer, modified SES-2002 has recently been replaced to a newly developed one, R4000-10 kV (GAMMADATA SCIENTA Co.), and the measurable KE has been extended from 6 to 10 keV. In addition to the analyzer, a motorized XYZΘ stage for a sample manipulator with a close-cycle He cryostat, two turbo molecular pumps, and CCD cameras are equipped with the measurement chamber. The whole system including load-lock and preparation chambers is mounted on a position adjustable stage, and is designed as compact as possible to carry the apparatus into the experimental hutch after preparing ultra high vacuum outside of the hutch. The vacuum of the measurement chamber is 10^{-8} Pa, and we can do low-temperature measurements down to 30 K.

3. Results and discussions

In order to check the basic performances of our system and to demonstrate the characteristics of HX–PES, we have measured core level and VB spectra of typical materials at 5.95 keV. It should be emphasized that no surface treatment was carried out and all the samples presented here were investigated as they were inserted.

Figs. 5(a) and (b) show HX–PES spectra of Au plate measured at 35 K. In the Au 4f core level (thick solid curve in (a)) and VB (thick solid curve

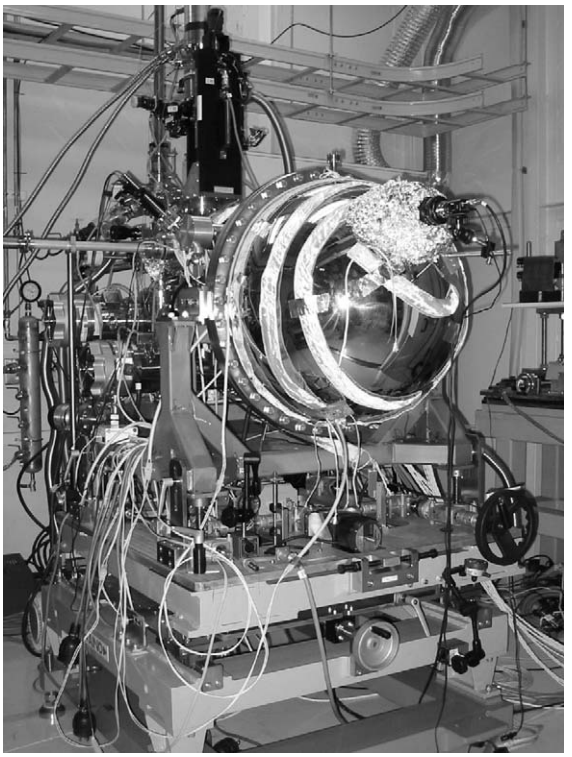

Fig. 4. Picture of the HX–PES apparatus placed in the experimental hutch at BL29XU in SPring-8.

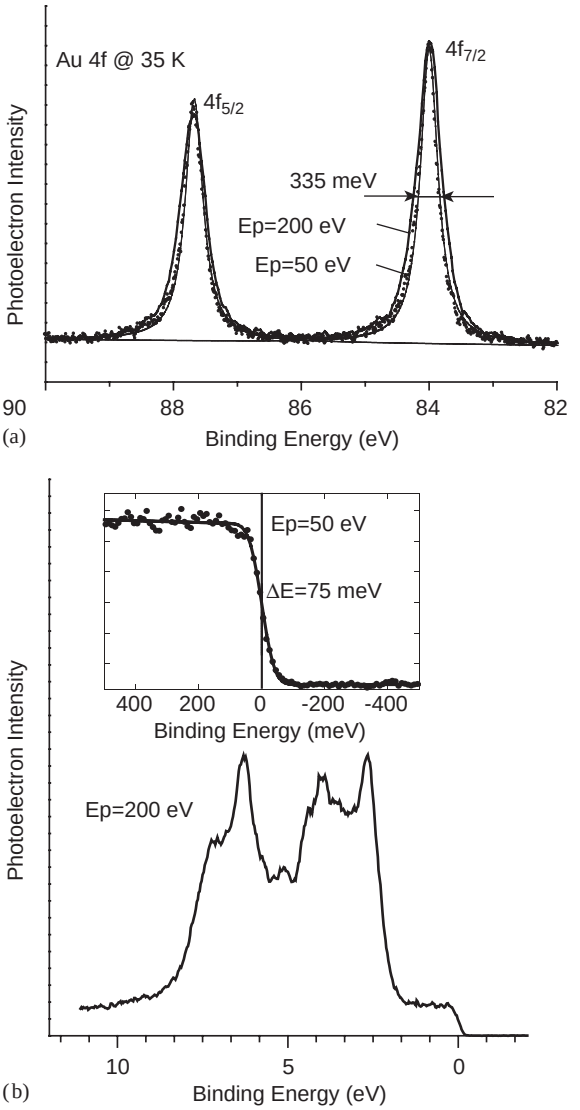

Fig. 5. (a) Au 4f and (b) VB photoelectron spectra of a Au plate measured at 35 K with 5.95 keV excitation. Thick solid curves in (a) and (b) were measured spectra with E_p of 200 eV in short accumulation times of 30 and 220 s, respectively. Dotted spectra in Au 4f (a) and in Fermi-edge profile (inset in (b)) were measured with $E_p = 50$ eV. The total energy resolution of 75 meV ($E/\Delta E = 79000$) was achieved for 5.95 keV photoelectrons. The dotted Au 4f spectrum can be fitted with pure Lorentz function (thin solid curve) with the FWHM of 335 meV.

in (b)) spectra measured with the pass energy (E_p) of 200 eV, the signal-to-noise ratios are very good even with short accumulation times of 30 and 220 s, respectively. The total instrumental energy resolution including the X-ray band width was 280 meV in this conventional setting. The inset in Fig. 5(b) shows the Fermi-edge profile at 35 K with $E_p = 50$ eV. The total energy resolution determined by fitting this profile is 75 ± 2 meV ($E/\Delta E = 79,000$) for 5.95 keV photoelectrons, and is comparable to the highest energy resolution of SX–PES. The dotted Au 4f spectrum in Fig. 5(a) was measured with the same energy resolution, and can be fitted with a pure Lorentz function (thin solid curve) with the FWHM of 335 meV, indicating the experimental resolution is much less than the life time broadening.

Next, to confirm the capability of the present method to probe bulk states of reactive surfaces, the VB spectra of a Si(1 0 0) surface with a thin-SiO_2 layer (0.58 nm) measured at room temperature are shown in Fig. 6. It is well known that the Si surface is easily oxidized even in vacuum.

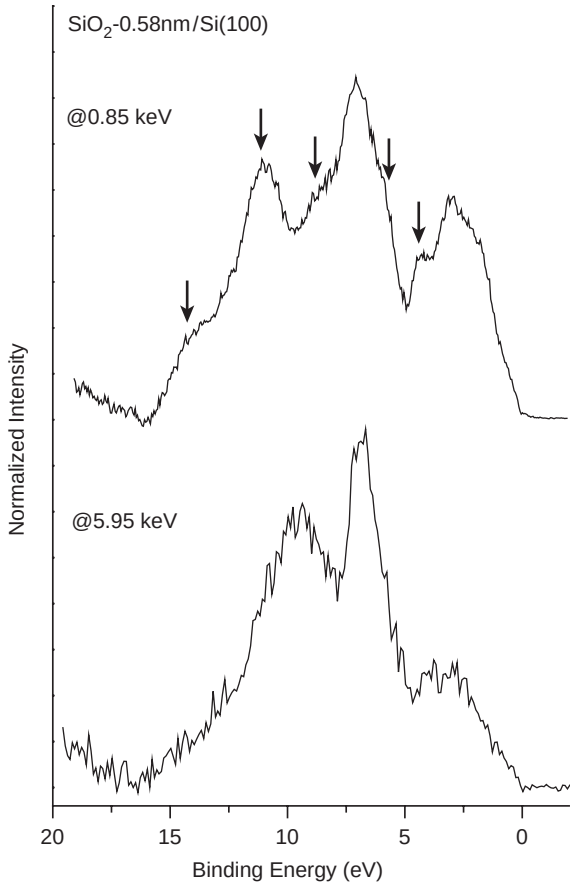

Fig. 6. VB–PES spectra of thin-SiO_2 layer (0.58 nm) on Si(1 0 0) measured at 5.95 keV (lower) and 0.85 keV (upper). Arrows indicate the structure originating from the surface SiO_2 layer.

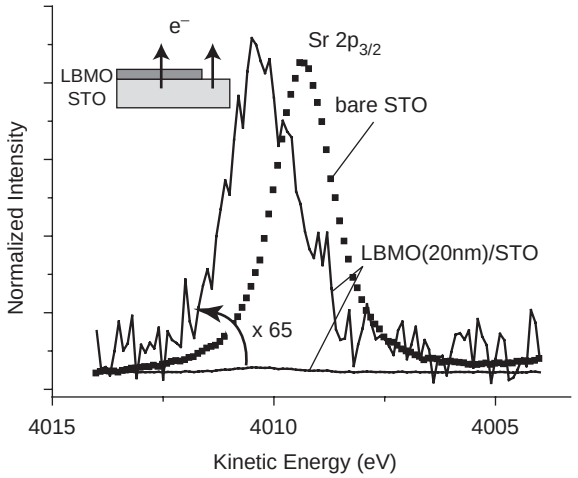

Fig. 7. Sr $2p_{3/2}$ core level spectra of bare SrTiO3 (STO) substrate and the substrate covered with a thin layer (20 nm) of $La0_{.85}Ba_{0.15}MnO_3$ (LBMO). The Sr $2p_{3/2}$ (binding energy:1940 eV) photoelectrons from the substrate with the KE of 4010 eV are still observable through the 20-nm-thick overlayer.

Comparing the HX (5.95 keV) spectrum with the SX (0.85 keV) spectrum, the structures marked by arrows in the SX spectrum, those are due to the thin surface layer of SiO_2, almost vanish in the HX spectrum. This result indicates negligible contribution of surface oxide layer of 0.58 nm thickness. The "surface insensitivity" of HX–PES enables us to investigate the intrinsic bulk state of thin films which are beyond the reach of "surface sensitive" PES because of lack of surface cleaning and preparation procedure.

In addition to "surface insensitivity", the large probing depth of HX–PES extends the applicability to embedded layers and interfaces in nanoscale buried layer system. Fig. 7 shows the Sr $2p_{3/2}$ spectra of a bare $SrTiO_3$ (STO) substrate and the substrate covered with a thin layer (20 nm) of $La_{0.85}Ba_{0.15}MnO_3$ (LBMO). The Sr $2p_{3/2}$ (binding energy:1940 eV) photoelectrons from the substrate with the KE of 4010 eV are still observable through the 20-nm-thick overlayer. The small KE difference between these two samples is attributed to band bending. From the intensity variation, the IMFP value of electrons with KE = 4010 eV in LBMO is estimated as 4 nm.

4. Conclusion

HX–PES with high throughput and high-energy resolution is realized for core level and VB studies using high-energy and high-brilliance SR at BL29XU in SPring-8. The high-energy resolution of 75 meV ($E/\Delta E = 79,000$) was achieved for 5.95 keV photoelectrons. The large probing depth at such high energies enables us to probe intrinsic bulk states and embedded layers without surface conditioning. New functional materials such as MBE-grown thin layers and various organic functional films, whose ideal surface cannot be prepared, are accessible directly after structural, electric and magnetic characterizations. We have

applied this method to high-k thin films [8], diluted magnetic semiconductors [9,16], compound semiconductors [17], and strongly correlated materials [18–24]. The combination of HX VB and core-level spectra will provide important information on electronic properties of various materials in the field of basic science and technologies.

This work was partially supported by the Ministry of Education, Science, Sports and Culture through a Grant-in-Aid for Scientific Research (A) (No. 15206006).

References

[1] S. Hüfner, Photoelectron Spectroscopy, Springer, Berlin-Hidelberg, 1995.
[2] The electron inelastic-mean-free-paths were estimated using NIST Standard Reference Database 71, "NIST Electron Inelastic-Mean-Free-Path Database: Ver. 1.1". It is distributed via the Web site http://www.nist.gov/srd/nist71.htm, and references therein.
[3] A. Sekiyama, T. Iwasaki, K. Matsuda, Y. Saitoh, S. Suga, Nature 403 (2000) 396.
[4] I. Lindau, P. Pianetta, S. Doniach, W.E. Spicer, Nature 250 (1974) 214.
[5] J.J. Yeh, I. Lindau, At. Data Nucl. Data Tables 32 (1985) 1.
[6] J. Danger, P. Le Fèvre, H. Magnan, D. Chandesris, S. Bourgeois, J. Jupille, T. Eickhoff, W. Drube, Phys. Rev. Lett. 88 (2002) 243001.
[7] W. Drube, Th. Eickhoff, H. Schulte-Schrepping, J. Heuer, AIP Conf. Proc. 705 (2004) 1130.
[8] K. Kobayashi, M. Yabashi, Y. Takata, T. Tokushima, S. Shin, K. Tamasaku, D. Miwa, T. Ishikawa, H. Nohira, T. Hattori, Y. Sugita, O. Nakatsuka, A. Sakai, S. Zaima, Appl. Phys. Lett. 83 (2003) 1005.
[9] Y. Takata, K. Tamasaku, T. Tokushima, D. Miwa, S. Shin, T. Ishikawa, M. Yabashi, K. Kobayashi, J.J. Kim, T. Yao, T. Yamamoto, M. Arita, H. Namatame, M. Taniguchi, Appl. Phys. Lett. 84 (2004) 4310.
[10] S. Thiess, C. Kunz, B.C.C. Cowie, T.-L. Lee, M. Renier, J. Zegenhagen, Solid State Commun. 132 (2004) 589.
[11] C. Dallera, L. Duò, L. Bricovich, G. Panaccione, G. Paolicelli, B. Cowie, J. Zegenhagen, Appl. Phys. Lett. 85 (2004) 4532.
[12] P. Torelli, et al., Rev. Sci. Instrum. 76 (2005) 023909.
[13] K. Tamasaku, Y. Tanaka, M. Yabashi, H. Yamazaki, N. Kawamura, M. Suzuki, T. Ishikawa, Nucl. Instr. and Meth. A 467/468 (2001) 686.
[14] H. Kitamura, J. Synchrotron Radiat. 7 (2000) 121.
[15] T. Ishikawa, K. Tamasaku, M. Yabashi, J. Synchrotron Radiat. 7 (2000) 121.
[16] J.J. Kim, H. Makino, K. Kobayashi, Y. Takata, T. Yamamoto, T. Hanada, M.W. Cho, E. Ikenaga, M. Yabashi, D. Miwa, Y. Nishino, K. Tamasaku, T. Ishikawa, S. Shin, T. Yao, Phys. Rev. B 70 (2004) R161315.
[17] K. Kobayashi, Y. Takata, T. Yamamoto, J.J. Kim, H. Makino, K. Tamasaku, M. Yabashi, D. Miwa, T. Ishikawa, S. Shin, T. Yao, Jpn. J. Appl. Phys. 43 (2004) L1029.
[18] A. Chainani, et al., Phys. Rev. B 69 (2004) R180508.
[19] K. Horiba, et al., Phys. Rev. Lett. 93 (2004) 236401.
[20] N. Kamakura, et al., Europhys. Lett. 68 (2004) 557.
[21] H. Sato, et al., Phys. Rev. Lett. 93 (2004) 246404.
[22] K. Yamamoto, et al., J. Phys. Soc. Japan 73 (2004) L2616.
[23] M. Taguchi, A. Chainani, N. Kamakura, K. Horiba, Y. Takata, M. Yabashi, K. Tamasaku, Y. Nishino, D. Miwa, T. Ishikawa, S. Shin, E. Ikenaga, T. Yokoya, K. Kobayashi, T. Mochiku, K. Hirata, K. Motoya, Phys. Rev. B 71 (2005) R155102.
[24] H. Tanaka, Y. Takata, K. Horiba, M. Taguchi, A. Chainani, S. Shin, D. Miwa, K. Tamasaku, Y. Nishino, T. Ishikawa, M. Awaji, A. Takeuchi, T. Kawai, K. Kobayashi, cond-mat/0410223.